HHS Public Access

Author manuscript

Am J Ophthalmol. Author manuscript; available in PMC 2021 January 01.

Published in final edited form as:

Am J Ophthalmol. 2020 January ; 209: 206–212. doi:10.1016/j.ajo.2019.09.004.

Detection of reduced retinal vessel density in eyes with geographic atrophy secondary to age-related macular degeneration using projection-resolved optical coherence tomography angiography

Qi Sheng You[1], **Jie Wang**[1,2], **Yukun Guo**[1], **Christina J. Flaxel**[1], **Thomas S. Hwang**[1], **David Huang**[1], **Yali Jia**[1,2], **Steven T. Bailey**[1]

[1]Casey Eye Institute, Oregon Health and Science University, Portland [2]Department of Biomedical Engineering, Oregon Health & Science University, Portland, OR 97239, USA

Abstract

Purpose: To compare retinal vessel density in eyes with geographic atrophy (GA) secondary to age-related macular degeneration (AMD) to age-matched healthy eyes using projection-resolved optical coherence tomography angiography (PR-OCTA).

Design: Prospective cross-sectional study.

Methods: Study participants underwent macular 3×3-mm OCTA scans with spectral domain OCTA. Reflectance-compensated retinal vessel densities were calculated on projection-resolved superficial vascular complex (SVC), intermediate capillary plexus (ICP), and deep capillary plexus (DCP). Quantitative analysis using normalized deviation compared the retinal vessel density in GA regions, 500 μm GA rim regions, and non-GA regions to similar macular locations in control eyes.

Results: Ten eyes with GA and 10 control eyes were studied. Eyes with GA had significantly lower vessel density in the SVC (54.8±2.4% vs. 60.8±3.1%, P<0.001), ICP (34.0±1.5% vs. 37.3±1.7%, P=0.003), and DCP (24.4±2.3% vs. 28.0±2.3%, P<0.001) compared to control eyes. Retinal vessel density within the GA region decreased significantly in SVC, ICP, and DCP. Retinal vessel density in the GA rim region decreased in SVC and ICP; but not in DCP. The non-GA region did not significantly deviate from normal controls. Eyes with GA had significantly reduced photoreceptor layer thickness; but similar nerve fiber layer, ganglion cell complex, inner nuclear layer, and outer plexiform layer thickness.

Corresponding Author: Steven T. Bailey, Casey Eye Institute, Oregon Health & Science University, 3375 SW Terwilliger Blvd, Portland, OR 97239. bailstev@ohsu.edu.

Conclusion: Eyes with GA have reduced retinal vessel density in SVC, ICP, and DCP compared to controls. Loss is greatest within regions of GA. Vessel density may be more sensitive than retinal layer thickness measurement in the detection of inner retinal change in eyes with GA.

Keywords

age-related macular degeneration; geographic atrophy; optical coherence tomography; angiography; vessel density

Introduction

Advanced age-related macular degeneration (AMD), in its neovascular and atrophic forms, is the leading cause of vision loss, particularly in industrialized countries.[1–3] Geographic atrophy (GA) causes a slow irreversible vision loss, accounting for approximately 20% of all cases of legal blindness in North America.[4] With the advent and success of anti-vascular endothelial growth factor for the treatment of neovascular AMD,[5–7] GA could become the leading cause of severe vision loss in the future.

GA is clinically characterized by sharply demarcated atrophic lesions of the outer retina and retinal pigment epithelium (RPE) with an increased visibility of underlying choroidal vessels.[4] Although GA primarily affects the outer retina, with loss of photoreceptors, retinal pigment epithelium (RPE) and the choriocapillaris; improved knowledge of inner retinal status in GA may be relevant for understanding the disease and developing potential therapies such as retinal prosthesis or stem cell therapy. Studies have previously demonstrated inner nuclear layer and ganglion cell loss in addition to outer retinal loss.[8,9] To the best of our knowledge, there has been no study quantifying inner retinal blood flow change in GA. Considering the secondary loss of inner retinal neurons, as evidenced by previous studies,[9,10] we hypothesize there may be change in perfusion in both the superficial and deep layer capillaries. OCTA provides an opportunity to quantify retinal perfusion non-invasively. However, traditional OCTA has limited vascular depth discrimination due to projection artifacts of superficial flow signal onto deeper layers.[11] The projection-resolved OCTA (PR-OCTA), developed by our group[12,13], improves vascular depth resolution by removing projection artifact while retaining *in-situ* flow signal from real blood vessels in deeper layers. PR-OCTA enables us to study the retinal vasculature within individual plexuses *in vivo* than previously possible.[12,14] The purpose of the current study is to evaluate inner retinal vessel density in the three retinal plexuses using PR-OCTA in eyes with GA.

Methods

This prospective clinical observational study adhered to the tenets of the Declaration of Helsinki and was conducted in compliance with the Health Insurance Portability and Accountability Act. The institutional review board at Oregon Health & Science University approved the study and written informed consent was obtained from each participant.

The inclusion criteria for GA patients were an age of 50+ years and diagnosis of GA secondary to AMD in at least one eye. GA was defined as sharply demarcated atrophic lesions of at least 175 μm with increased visibility of choroidal vessels. The diagnosis of GA

was confirmed by both hypoautofluorescence on fundus autofluorescence (FAF) image and OCT scans (Spectralis, Heidelberg, Germany) demonstrating congruent loss of photoreceptors and RPE, and hypertransmission of OCT signal into the choroid. A group of age matched healthy participants was included as control. The inclusion criteria of controls were an age of at least 50 years, no history of retinal diseases, corrected visual acuity ≥20/20, intraocular pressure <21mmHg and absence of any abnormalities on clinical fundus examination and OCT. The exclusion criteria for both GA and control groups included a history of diabetes mellitus, choroidal or retinal neovascularization, previous intraocular surgery except cataract surgery, any other macular disease such as epiretinal membrane or vitreomacular traction syndrome, refractive error greater than −6 or +3 diopters and media opacities that preclude a high-quality OCTA scan.

All participants underwent a comprehensive ocular examination, including early treatment of diabetic retinopathy study (ETDRS) visual acuity testing, intraocular pressure, axial length measurement (IOL master 500, Carl Zeiss Meditec, Dublin, California, USA), dilated fundus examination, fundus photography (Zeiss FF450 plus, Carl Zeiss Meditec, Dublin, California, USA), OCTA, FAF (Spectralis HRA+OCT; Heidelberg Engineering, Heidelberg, Germany), structural OCT as well as a systemic blood pressure measurement. The mean arterial pressure (MAP) was calculated as the diastolic blood pressure plus one-third of the difference between the diastolic blood pressure and the systolic blood pressure. The ocular perfusion pressure (OPP) was determined by subtracting the intraocular pressure (IOP) from the two-thirds of MAP.

OCTA was obtained after pupil dilation using a commercially available spectral-domain instrument, RTVue XR Avanti (Optovue, Inc.), with a center wavelength of 840 nm and an axial scan rate of 70-kHz. The 3×3-mm scans centered at the fovea were acquired. The commercial version of split-spectrum amplitude decorrelation angiography (SSADA) algorithm[15] was used to detect blood flow by comparing consecutive B-scans at the same location. Each scan set consists of one vertical-priority raster and one horizontal-priority raster scan. The AngioVue software uses an orthogonal registration algorithm to register the two perpendicular raster volumes to produce a merged 3D OCT angiogram. The merged volumetric angiograms were then exported for custom processing using COOL-ART software[16]. Scans were excluded if images were out of focus, significant motion artifacts were detected, or signal strength index (SSI) was less than 55.

A semi-automated algorithm based on directional graph search segmented the volumes.[16,17] Segmentations were then reviewed and manually adjusted to ensure accuracy. Retinal layer thickness measurements were defined by the following: the whole retinal layer - from internal limiting membrane (ILM) to inner surface of RPE; nerve fiber layer (NFL) - from ILM to outer surface of NFL; ganglion cell complex (GCC) consisting of both ganglion cell layer and inner plexiform layer (IPL) - from outer surface of NFL to inner surface of inner nuclear layer (INL); inner nuclear layer - from inner surface of INL to outer surface of INL; outer plexiform layer (OPL) - from outer surface of INL to inner surface of outer nuclear layer (ONL); photoreceptor thickness - from inner surface of ONL to inner surface of RPE. Retinal vessel density was defined as the proportion of vessel area with blood flow over the total area measured. Reflectance compensated vessel densities were calculated on

projection-resolved superficial vascular complex (SVC), intermediate capillary plexus (ICP), and deep capillary plexus (DCP)[12,13,18]. The central 0.6-mm diameter area centered on the fovea was excluded to limit the effect of foveal avascular zone on vessel density measurement[19–22]. *En face* OCT reflectance map was used to identify areas of GA.

Retinal vessel densities were calculated within GA regions, within GA rim region (500 μm rim around GA), and in non-GA regions that included regions outside of GA rim area.[23] For eyes with multiple GA regions, a mean vessel density of all GA regions or rim area was calculated by dividing the sum of vessel area within GA region or rim area by the total GA area or total rim area. Considering that GA location varies between individuals and that vessel density varies by location within the macula[14], we calculated fractional vessel density deviation maps normalized to the average vessel density map in the normal control group. The normalized vessel deviation was defined as the value from the eye under evaluation minus the normal average, then divided by the normal average. Thus the reduction of vessel density within GA rims could be calculated by averaging the normalized vessel density deviation in the rim area. The analytic areas were centered on the foveal avascular zone and adjusted for transverse optical magnification calculated according to the axial length of each eye. Pixel coordinate was used to match the location when comparing GA region, GA rim and non-GA region to corresponding areas of normal average maps.

Statistical analysis was conducted using Statistical Package for Social Sciences software (SPSS for Windows, version 25.0; IBM SPSS Inc., Chicago, USA). Descriptive statistics included mean, standard deviation (SD), range, and percentages were presented where appropriate. Shapiro-Wilk was used to test normality of data distribution of age, axial length, retinal layer thickness and vessel density. Independent sample *t* test was used to compare age, axial length, retinal thickness, and vessel density on each individual plexus between eyes with GA and healthy normal eyes. Pearson correlation was used to analyze the correlation between extent of vessel density reduction and GA size, and the correlation between vessel densities and retinal layer thicknesses. A one-sample t test was used to determine whether the normalized deviation is significantly different from zero within GA region, GA rims and outside GA rim region. All P values were 2-sided and considered statistically significant if the value was less than 0.05. Bonferroni correction was applied when doing multiple comparisons.

Results

One eye each of 10 GA patients (7 women) and 10 normal healthy controls (7 women) were included. The mean ages were 81.3±9.3 (range: 66–95 years) and 76.3±4.2 years (range: 73–85 years) for GA and control groups respectively (P=0.14). The axial length was not significantly different between GA and control eyes (24.02±0.63 vs. 24.63±0.85mm, P=0.09). The systolic arterial blood pressure, diastolic blood pressure, intraocular pressure and calculated OPP was similar between the two groups. On the 3×3-mm OCTA scan area, GA lesion was multifocal in 9/10 eyes and monofocal in 1/10 eyes. The mean atrophic area was 1.84±1.00 mm^2 (range 0.72–4.35 mm^2) on 3×3-mm *en face* OCT scans. Table 1 summarizes the clinical characteristics of the participants.

The mean retinal vessel densities were significantly lower in GA eyes compared to normal controls in SVC (54.8±2.4 % vs. 60.8±3.1%, P<0.001), ICP (34.0±1.5% vs. 37.3±1.7%, P<0.001) and DCP (24.4 ± 2.3% vs. 28.0 ± 2.3%, P=0.002). The DCP in eyes with GA had the greatest reduction (13%) of retinal vessel density compared to the DCP of normal controls, followed by the SVC (10%) and ICP (9%). The GA size was not significantly associated with the extent of vessel density reduction in SVC (P=0.24), ICP (P=0.31), or DCP (P=0.59).

Quantitative analysis using normalized deviation compared the retinal vessel density in GA regions, GA rim regions and non-GA regions to similar macular locations in control eyes (Table 2). The retinal vessel density within the GA region was significantly lower in SVC, ICP, and DCP. Retinal vessel density in the GA rim region decreased in only the SVC and ICP, but not in DCP. The non-GA region did not deviate from normal controls. The GA region had the greatest reduction in retinal vessel density (figure 1).

Compared to normal controls, eyes with GA had significantly reduced whole retinal layer thickness (254.3±9.6 vs. 272.4±12.4 μm, P=0.002) and photoreceptor layer thickness (90.2±12.1 vs. 110.0±10.1 μm, P=0.001). There was no difference in NFL (26.0± 2.8 vs. 24.4 ± 3.3 μm, P=0.23), GCC (73.9±4.4 vs. 76.3±5.3 μm, P=0.28), INL (36.5± 4.3 vs. 37.5±2.3 μm, P=0.55), and OPL thickness (27.6 ± 3.5 vs. 24.3±4.7 μm, P=0.09) (Table 3).

Quantitative analysis using normalized deviation compared retinal layer thickness in GA regions, GA rim regions, and non-GA regions to similar macular locations in control eyes (Table 3). Within GA regions had significantly reduced photoreceptor layer thickness and reduced all-layer retinal thickness. OPL thickness was increased and there was no thickness change in NFL, GCC and INL. Normalized deviation analysis in GA rims demonstrated significantly reduced thickness in the photoreceptor layer and all-layer retina, but no significant thickness change in NFL, GCC, INL and OPL. In non-GA region, photoreceptor thickness was significantly reduced and there was no change in the other layers or all-layer retina.

Discussion

In this study, we demonstrated a significant decrease (9–13% reduction) in retinal vessel densities in all the three retinal plexuses in GA eyes compared to age-matched normal controls. The reduced retinal vessel density is likely associated with the significant loss of photoreceptors and ganglion cells as previously demonstrated in histopathologic studies of GA secondary to AMD. Kim et al. studied 10 GA eyes and 5 normal control eyes histomorphometrically, demonstrating 76.9% (P<0.0001) reduction of ONL cells and 30% (P=0.0008) loss of ganglion cells in GA eyes compared to control eyes.[10] Among GA eyes, the nuclei in all three layers were significantly reduced in segments in which the retinal pigment epithelium was completely absent.[10] The authors suggested trans-synaptic neuronal degeneration leads to secondary loss of ganglion cells due to chronically reduced input from photoreceptor loss. An experimental study in non-human primates demonstrated that macular focal laser induced RPE and photoreceptor destruction leads to subsequent retinal capillary closure 1 and 5 months later.[24] Our current study used PR-OCTA to demonstrate *in*

vivo retinal vessel density loss in all 3 retinal plexuses, in addition to photoreceptor loss, in eyes with GA secondary to AMD.

An alternative explanation for the decrease of retinal vessel density in GA eyes is the potential increased oxygen flow from choroid to inner retina. The atrophy of RPE and photoreceptors, which normally consume large amounts of oxygen, could allow more of the oxygen from the choroid to diffuse to the inner half of the retina, which in turn could lead to a constriction of retinal vasculature. This is similar to the effect of panretinal photocoagulation on the inner retina.[25–27] However, one major difference is that choriocapillaris is compromised in GA eyes. It is unclear whether there could be increase of diffusion of oxygen to inner retina from the deeper choroidal vascular layers, which have been shown to rise to the level of Bruch's membrane in these eyes.[28]

Our findings of reduced photoreceptor thickness in GA are consistent with prior studies[9,10]. However, we did not find inner retinal layer thickness changes, which was reported in other studies. Using spectral-domain OCT with manual segmentations, Ramkumar et al found a 16% ganglion cell volume loss in GA eyes compared to age-matched controls.[9] Our methodology differed from this study. Because the reflectivity of the ganglion cell layer and IPL is similar, we were unable to reliably segment between these layers, and we reported the combined thickness of IPL and ganglion cell layer as the GCC; instead of reporting a separate ganglion cell layer thickness. Zucchiatti et al employed spectral domain OCT (Cirrus HD-OCT) to automatically measure ganglion cell complex (GCC) in different stages of AMD patients, among whom 26 were GA patients. The authors found a significant 37% GCC loss in GA eyes compared to controls.[8] In this study there was no mention of manual segmentation and this may have resulted in segmentation errors. The automated segmentations in all the ten GA eyes in our study were manually reviewed and adjusted to improve accuracy. Additional possible explanations for discrepancies include each study used different instruments and study population may have had variations. For example, eyes with greater duration of disease and larger areas of GA may have a greater degree inner retinal degeneration.

Despite the non-significant inner retinal thickness change in GA eyes compared to normal controls, we found a significant retinal vessel density decrease in all three plexuses in GA eyes, suggesting vessel density measurement by OCTA might be more sensitive than structural thickness measurement for the detection of inner retinal changes in GA. One explanation for the paradoxical finding of a decrease in vessel density without decrease in thickness in inner retinal layers in GA region is that the inner retinal neurons were retained in our cases, but their perfusion was reduced due to reduced metabolism from reduced synaptic activity secondary to loss of photoreceptors. Another possibility is that the inner retinal neurons were reduced in number but the volume or thickness was made up by increased glial volume or extracellular matrix. It is also understandable that the biggest reduction happened in DCP among the three plexuses in GA eyes, since the synaptic activity in the OPL should be reduced when there is photoreceptor atrophy.

Recent studies with optical coherence tomography angiography (OCTA) found significant impairment of choriocapillaris flow within GA region and surrounding GA area, suggesting

choriocapillaris blood flow alterations may be associated with the development and progression of GA.[23,29–35] Our study detected reduced retinal vessel density in all layers within GA. Interestingly, we noted reduced SVC and ICP in GA rim areas, but not in DCP. A possible explanation for the reduced SCV and ICP, but not DCP in the GA rim area is because ganglion cell in the rim have receptive fields that include photoreceptors in the GA region. This could in theory result in reduced inner retinal metabolic demand in the GA rim area and subsequent reduced SVC and ICP blood flow. Because photoreceptors persist in the GA rim area, there is persistent metabolic demand for continued DCP blood flow. The lack of DCP reduction in the rim suggest that the reduction in retinal circulation might be a sequelae rather than a cause of GA. The fact that photoreceptor thickness is reduced in the rim suggests that photoreceptor atrophy could be part of the causal chain in GA, and could be consistent with roles played by the RPE and choriocapillaris. Further study is needed to better understand the inner retinal blood flow in the pathogenesis of GA.

Currently, there is no treatment available for GA. Efforts to replace photoreceptors with stem cells or retinal prosthesis are under study. Given we found only a 9–13% reduction in retinal vessel density even with significant loss of outer retinal photoreceptors in the atrophic area, there may be adequate inner retinal blood flow to support ganglion cell function following photoreceptor replacement or following stimulation by a retinal prosthesis. OCTA may be a useful biomarker to assess if there is increased inner retinal blood flow changes following therapeutic intervention.

Limitations of the study include the cross-sectional design and relative small sample size. A longitudinal study with a larger sample size is needed to confirm our findings and to test whether the vessel density loss precedes retinal thinning. Despite the limitations, to the best of our knowledge, this is the first study on vessel density of three retinal capillary plexuses in GA eyes and may enrich the knowledge of natural history of GA.

In conclusion, quantifying vessel density using PR-OCTA demonstrated reduced perfusion in all three retinal plexuses (SVC, ICP and DCP) in eyes with GA compared to normal age-matched controls. Vessel density loss was greatest within regions of GA. OCTA measured vessel density may be more sensitive than thickness measurement in detection of inner retinal changes in GA eyes.

Acknowledgements/Disclosure:

a. Funding/Support: The study was supported by grants R01 EY024544, R01 EY027833, and P30 EY010572 from the National Institutes of Health, an unrestricted departmental funding grant and William & Mary Greve Special Scholar Award from Research to Prevent Blindness, New York. The funding source had no role in the design and conduct of the study; collection, management, analysis, and interpretation of the data; preparation, review, or approval of the manuscript; and decision to submit the manuscript for publication.

b. Financial disclosure: Oregon Health & Science University (OHSU) and Drs. Jia and Huang have a significant financial interest in Optovue Inc, a company that may have a commercial interest in the results of this research and technology. These potential conflicts of interest have been reviewed and managed by OHSU. No other disclosures were reported.

References

1. Flaxman SR, Bourne RRA, Resnikoff S, et al. Global causes of blindness and distance vision impairment 1990–2020: a systematic review and meta-analysis. Lancet Glob Health 2017; 5(12): e1221–e34. [PubMed: 29032195]
2. Jonas JB, Cheung CMG, Panda-Jonas S. Updates on the Epidemiology of Age-Related Macular Degeneration. Asia Pac J Ophthalmol (Phila) 2017; 6(6): 493–7. [PubMed: 28906084]
3. Wong WL, Su X, Li X, et al. Global prevalence of age-related macular degeneration and disease burden projection for 2020 and 2040: a systematic review and meta-analysis. Lancet Glob Health 2014; 2(2): e106–16. [PubMed: 25104651]
4. Holz FG, Strauss EC, Schmitz-Valckenberg S, van Lookeren Campagne M. Geographic atrophy: clinical features and potential therapeutic approaches. Ophthalmology 2014; 121(5): 1079–91. [PubMed: 24433969]
5. Brown DM, Kaiser PK, Michels M, et al. Ranibizumab versus verteporfin for neovascular age-related macular degeneration. N Engl J Med 2006; 355(14): 1432–44. [PubMed: 17021319]
6. Rosenfeld PJ, Brown DM, Heier JS, et al. Ranibizumab for neovascular age-related macular degeneration. N Engl J Med 2006; 355(14): 1419–31. [PubMed: 17021318]
7. Martin DF, Maguire MG, Ying GS, Grunwald JE, Fine SL, Jaffe GJ. Ranibizumab and bevacizumab for neovascular age-related macular degeneration. N Engl J Med 2011; 364(20): 1897–908. [PubMed: 21526923]
8. Zucchiatti I, Parodi MB, Pierro L, et al. Macular ganglion cell complex and retinal nerve fiber layer comparison in different stages of age-related macular degeneration. Am J Ophthalmol 2015; 160(3): 602–7.e1. [PubMed: 26052088]
9. Ramkumar HL, Nguyen B, Bartsch DU, et al. REDUCED GANGLION CELL VOLUME ON OPTICAL COHERENCE TOMOGRAPHY IN PATIENTS WITH GEOGRAPHIC ATROPHY. Retina 2018; 38(11): 2159–67. [PubMed: 29117065]
10. Kim SY, Sadda S, Humayun MS, de Juan E Jr., Melia BM, Green WR. Morphometric analysis of the macula in eyes with geographic atrophy due to age-related macular degeneration. Retina 2002; 22(4): 464–70. [PubMed: 12172114]
11. Spaide RF, Fujimoto JG, Waheed NK. IMAGE ARTIFACTS IN OPTICAL COHERENCE TOMOGRAPHY ANGIOGRAPHY. Retina 2015; 35(11): 2163–80. [PubMed: 26428607]
12. Wang J, Zhang M, Hwang TS, et al. Reflectance-based projection-resolved optical coherence tomography angiography [Invited]. Biomed Opt Express 2017; 8(3): 1536–48. [PubMed: 28663848]
13. Zhang M, Hwang TS, Campbell JP, et al. Projection-resolved optical coherence tomographic angiography. Biomed Opt Express 2016; 7(3): 816–28. [PubMed: 27231591]
14. Campbell JP, Zhang M, Hwang TS, et al. Detailed Vascular Anatomy of the Human Retina by Projection-Resolved Optical Coherence Tomography Angiography. Sci Rep 2017; 7: 42201. [PubMed: 28186181]
15. Jia Y, Tan O, Tokayer J, et al. Split-spectrum amplitude-decorrelation angiography with optical coherence tomography. Opt Express 2012; 20(4): 4710–25. [PubMed: 22418228]
16. Zhang M, Wang J, Pechauer AD, et al. Advanced image processing for optical coherence tomographic angiography of macular diseases. Biomed Opt Express 2015; 6(12): 4661–75. [PubMed: 26713185]
17. Guo Y, Camino A, Zhang M, et al. Automated segmentation of retinal layer boundaries and capillary plexuses in wide-field optical coherence tomographic angiography. Biomed Opt Express 2018; 9(9): 4429–42. [PubMed: 30615747]
18. Gao SS, Jia Y, Liu L, et al. Compensation for Reflectance Variation in Vessel Density Quantification by Optical Coherence Tomography Angiography. Invest Ophthalmol Vis Sci 2016; 57(10): 4485–92. [PubMed: 27571015]
19. Wei E, Jia Y, Tan O, et al. Parafoveal retinal vascular response to pattern visual stimulation assessed with OCT angiography. PLoS One 2013; 8(12): e81343. [PubMed: 24312549]

20. Zang P, Liu G, Zhang M, et al. Automated motion correction using parallel-strip registration for wide-field en face OCT angiogram. Biomed Opt Express 2016; 7(7): 2823–36. [PubMed: 27446709]
21. Hwang TS, Gao SS, Liu L, et al. Automated Quantification of Capillary Nonperfusion Using Optical Coherence Tomography Angiography in Diabetic Retinopathy. JAMA Ophthalmol 2016; 134(4): 367–73. [PubMed: 26795548]
22. Hwang TS, Hagag AM, Wang J, et al. Automated Quantification of Nonperfusion Areas in 3 Vascular Plexuses With Optical Coherence Tomography Angiography in Eyes of Patients With Diabetes. JAMA Ophthalmol 2018; 136(8): 929–36. [PubMed: 29902297]
23. Nassisi M, Shi Y, Fan W, et al. Choriocapillaris impairment around the atrophic lesions in patients with geographic atrophy: a swept-source optical coherence tomography angiography study. Br J Ophthalmol 2019; 103(7): 911–7. [PubMed: 30131381]
24. Wilson DJ, Finkelstein D, Quigley HA, Green WR. Macular grid photocoagulation. An experimental study on the primate retina. Arch Ophthalmol 1988; 106(1): 100–5. [PubMed: 3337683]
25. Budzynski E, Smith JH, Bryar P, Birol G, Linsenmeier RA. Effects of photocoagulation on intraretinal PO2 in cat. Invest Ophthalmol Vis Sci 2008; 49(1): 380–9. [PubMed: 18172116]
26. Grunwald JE, Riva CE, Brucker AJ, Sinclair SH, Petrig BL. Effect of panretinal photocoagulation on retinal blood flow in proliferative diabetic retinopathy. Ophthalmology 1986; 93(5): 590–5. [PubMed: 3725318]
27. Feke GT, Green GJ, Goger DG, McMeel JW. Laser Doppler measurements of the effect of panretinal photocoagulation on retinal blood flow. Ophthalmology 1982; 89(7): 757–62. [PubMed: 6889717]
28. Nesper PL, Lutty GA, Fawzi AA. RESIDUAL CHOROIDAL VESSELS IN ATROPHY CAN MASQUERADE AS CHOROIDAL NEOVASCULARIZATION ON OPTICAL COHERENCE TOMOGRAPHY ANGIOGRAPHY: Introducing a Clinical and Software Approach. Retina 2018; 38(7): 1289–300. [PubMed: 29059100]
29. Choi W, Moult EM, Waheed NK, et al. Ultrahigh-Speed, Swept-Source Optical Coherence Tomography Angiography in Nonexudative Age-Related Macular Degeneration with Geographic Atrophy. Ophthalmology 2015; 122(12): 2532–44. [PubMed: 26481819]
30. Dansingani KK, Freund KB. Optical Coherence Tomography Angiography Reveals Mature, Tangled Vascular Networks in Eyes With Neovascular Age-Related Macular Degeneration Showing Resistance to Geographic Atrophy. Ophthalmic Surg Lasers Imaging Retina 2015; 46(9): 907–12. [PubMed: 26469229]
31. Kvanta A, Casselholm de Salles M, Amren U, Bartuma H. OPTICAL COHERENCE TOMOGRAPHY ANGIOGRAPHY OF THE FOVEAL MICROVASCULATURE IN GEOGRAPHIC ATROPHY. Retina 2017; 37(5): 936–42. [PubMed: 27533772]
32. Moult EM, Waheed NK, Novais EA, et al. SWEPT-SOURCE OPTICAL COHERENCE TOMOGRAPHY ANGIOGRAPHY REVEALS CHORIOCAPILLARIS ALTERATIONS IN EYES WITH NASCENT GEOGRAPHIC ATROPHY AND DRUSEN-ASSOCIATED GEOGRAPHIC ATROPHY. Retina 2016; 36 Suppl 1: S2–s11. [PubMed: 28005659]
33. Sacconi R, Corbelli E, Carnevali A, Querques L, Bandello F, Querques G. OPTICAL COHERENCE TOMOGRAPHY ANGIOGRAPHY IN GEOGRAPHIC ATROPHY. Retina 2018; 38(12): 2350–5. [PubMed: 29016457]
34. Waheed NK, Moult EM, Fujimoto JG, Rosenfeld PJ. Optical Coherence Tomography Angiography of Dry Age-Related Macular Degeneration. Dev Ophthalmol 2016; 56: 91–100. [PubMed: 27023214]
35. Corbelli E, Sacconi R, Rabiolo A, et al. Optical Coherence Tomography Angiography in the Evaluation of Geographic Atrophy Area Extension. Invest Ophthalmol Vis Sci 2017; 58(12): 5201–8. [PubMed: 29049720]

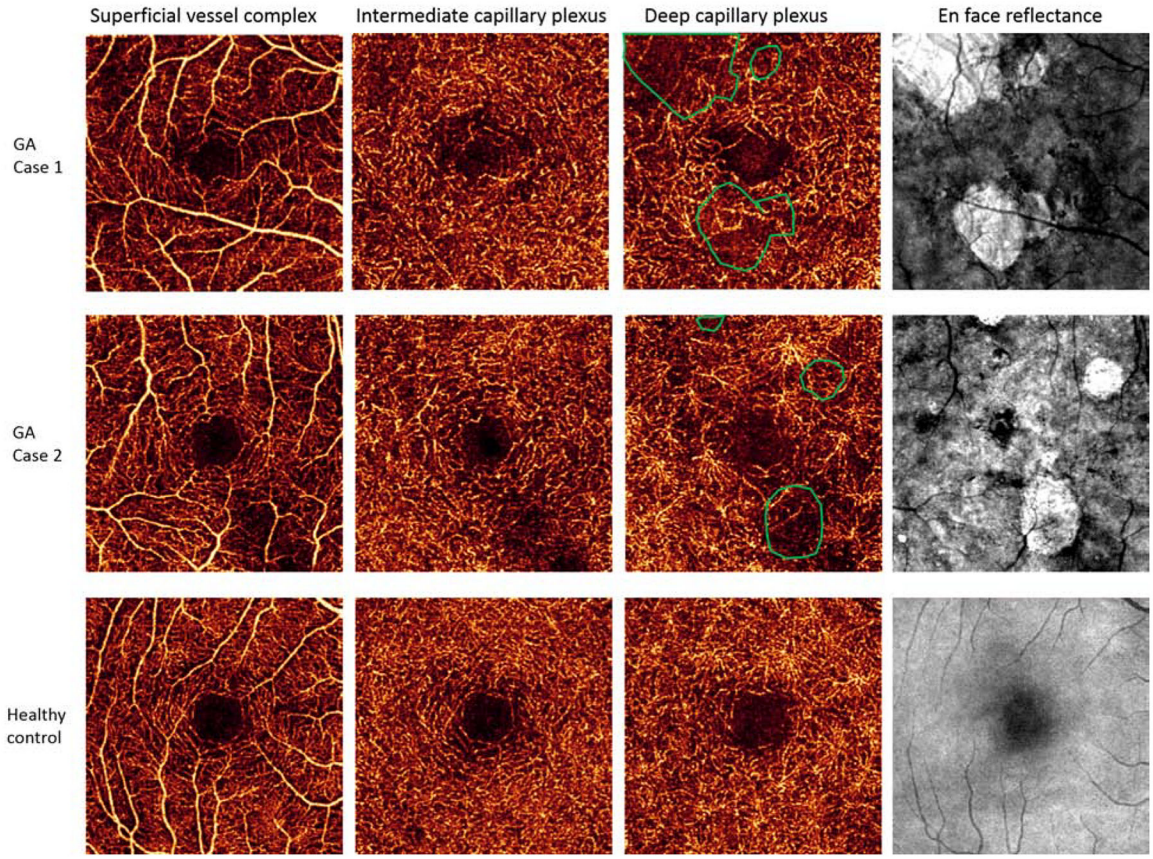

Figure 1.

Retinal vessel density is reduced in superficial vessel complex, intermediate capillary plexus and deep capillary plexus in two eyes with geographic atrophy compared to a healthy age-matched control. Retinal vessel density loss was greatest within regions of geographic atrophy (green circles).

Table 1.

Clinical characteristics of study participants with geographic atrophy secondary to age-related macular degeneration and age-matched controls.

Parameters	Healthy control (n=10) Mean (standard deviation)	GA patients (n=10) Mean (standard deviation)	P value
Age (years)	76.3 (4.2)	81.3 (9.3)	0.14
Sex(male/female)	7/3	7/3	1.00
Axial length (mm)	24.62 (0.85)	24.02 (0.63)	0.09
Intraocular pressure (mmHg)	14.8(2.4)	13.8(2.8)	0.41
Visual acuity (ETDRS letters)	85.7(2.1)	73.1(7.0)	<0.001
Systolic Blood pressure (mmHg)	126.2(18.7)	130.2(18.4)	0.67
Diastolic blood pressure (mmHg)	74.4(11.1)	74.4(10.8)	1.00
Ocular perfusion pressure (mmHg)	46.4(8.2)	48.2(6.4)	0.59

GA: geographic atrophy; ETDRS: early treatment diabetic retinopathy study; OCTA: optical coherence tomography angiography

Table 2.

Retinal vessel density in eyes with geographic atrophy and age-matched controls.

Layers	VD (SD) % in control eyes (n=10)	VD (SD) % in GA eyes (n=10)	P value	Normalized VD deviation of GA region	P value (compared to 0)	Normalized VD deviation of GA rims	P value (compared to 0)	Normalized VD deviation of non-GA region	P value (compared to 0)
SVC	60.76 (3.10)	54.80 (2.37)	<0.001	−0.12	0.005	−0.09	0.003	0.03	0.49
ICP	37.29 (1.71)	34.01 (1.53)	<0.001	−0.20	0.001	−0.06	0.01	0.05	0.40
DCP	28.04 (2.26)	24.39 (2.26)	0.002	−0.32	<0.001	0.01	0.83	0.34	0.09

GA: geographic atrophy; AMD: age-related macular degeneration; SVC: superficial vascular complex; ICP: intermediate capillary plexus; DCP: deep capillary plexus; VD: vessel density; SD: standard deviation.

Table 3

Retinal layer thickness in eyes with geographic atrophy and age-matched controls

Retina layers	Healthy Control eyes (SD) μm	GA eyes (SD) μm	P value	Normalized deviation of thickness in GA region	P value (compared to 0)	Normalized deviation of thickness in GA rims	P value (compared to 0)	Normalized deviation of thickness in non-GA region	P value (compared to 0)
NFL	24.4 (3.2)	26.0 (2.8)	0.23	0.10	0.29	0.04	0.52	0.08	0.18
GCC	76.3 (5.3)	73.9 (4.4)	0.27	0.01	0.79	−0.03	0.17	0.00	0.92
INL	37.5 (2.3)	36.5 (4.3)	0.55	0.002	0.96	−0.05	0.25	−0.02	0.64
OPL	24.3 (4.7)	27.6 (3.5)	0.09	0.22	0.006	0.11	0.06	0.14	0.08
Photoreceptor	110.0 (10.1)	90.2 (12.1)	0.001	−0.64	<0.001	−0.35	<0.001	−0.19	0.03
Whole retina	272.4 (12.4)	254.3 (9.6)	0.002	−0.15	<0.001	−0.08	<0.001	−0.02	0.14

NFL: nerve fiber layer; GCC: ganglion cell layer complex, including ganglion cell body layer and inner plexiform layer; INL: inner nuclear layer; OPL: outer plexiform layer; SD: standard deviation; GA: geographic atrophy